



Simulations of resonant magnetic scattering from FeRh films

Gaynanov Bulat

NRNU „MEPhI“

Supervisors: Ruslan Kurta, Andreas Scherz

European XFEL, DESY, Hamburg

September 8, 2015

Content

- 1. Introduction: ultrafast generation of magnetic order in FeRf films.**
- 2. Resonant magnetic x-ray scattering.**
- 3. Monte-Carlo simulations of magnetic FeRh films.**
- 4. Results of simulations.**
 - 4.1 Ising model.
 - 4.2 Bubble-domain model.
- 5. Conclusions.**
- 6. References.**

1. Introduction: ultrafast generation of magnetic order in FeRh films

FeRh is a prototypical system for the solid-state first order phase transition where the magnetization is the order parameter (fig.1). The generation of FM order in FeRh on ultrashort time scales much faster than the recovery of the magnetization from laser-heating in other systems is an appealing idea (fig.2). The possibility to further tailor the speed of the AFM-FM phase switching by nanostructuring the material makes FeRh a potential candidate for ultrafast heat assisted magnetic recording.

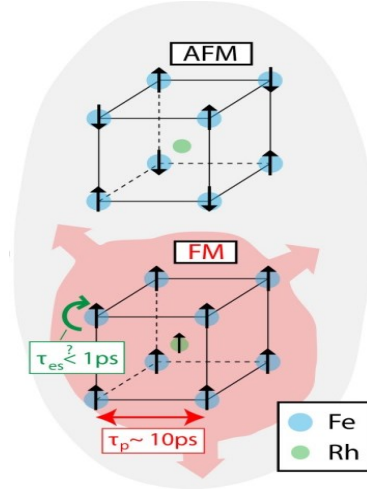


Figure 1 FeRh magnetic moments in the AF and F states.

The ultrafast antiferromagnetic (AFM) to ferromagnetic (FM) transition in FeRh films has been studied in x-ray diffraction and all-optical pump-probe experiments using transient reflectivity and time-resolved magneto-optical Kerr effect (tr-MOKE) [1,2]. While the reflectivity measures a combination of electronic and structural properties, tr-MOKE measures the magnetization.

Time-resolved all-optical pump-probe magneto-optical Kerr effect (tr-MOKE) measurements suggest an ultrafast FM response indicative of an electronically driven phase transition on sub-picosecond (ps) time scales [1]. The electronic AFM to FM transition is accompanied by an isotropic lattice expansion in the bulk, thus when monitoring the lattice expansion using hard x-ray diffraction, nucleation and growth of regions exhibiting the FM phase lattice parameters were observed on 10ps time-scales.

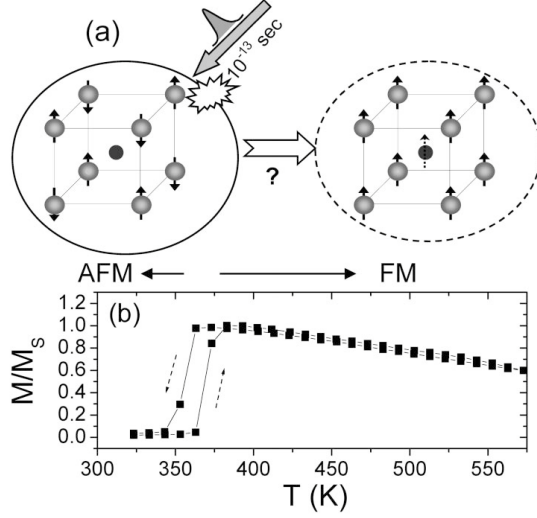


Figure 2 (a) Schematic of the ultrafast generation of ferromagnetic order by inducing an AFM-FM transformation in FeRh when excited with femtosecond optical pulses. (b) Temperature dependence of the saturation magnetization of the annealed 100-nm-thick FeRh film.

The aim of our study is to derive a simple model that describes the evolution of the structure and magnetization of FeRh films on ultrashort timescales, measured in resonant magnetic x-ray scattering experiments at LCLS.

2. Resonant magnetic x-ray scattering

X-ray resonant magnetic scattering (XRMS) makes use of the resonant enhancement of the magnetic scattering occurring at an absorption edge. For instance, in the case of the $L_{2(3)}$ edges in a transition metal, it results from the electric dipole transition from the $2p_{1/2(3/2)}$ atomic core level towards the unoccupied $3d_{3/2(5/2)}$ states which carry the magnetic moment. As for x-ray magnetic circular dichroism (XMCD), the magnetic sensitivity arises from the exchange splitting of the unoccupied 3d states induced by their magnetic polarization, and from the spin polarization of the photoelectron which is related to the spin—orbit coupling in the 2p core level [4, 5].

Intensity scattered from magnetic system at resonant conditions can be expressed as

$$I(k) = A \sum_{j,t} F_a^{j*}(k, E) F_b^t(k, E) e^{ikR_{jt}} \quad (1)$$

where the atomic scattering factor (neglecting weak term related to the linear magnetic dichroism) can be written as

$$F(k, E) = -(e_f \cdot e_i) f(k, E) - i[e_f \times e_i] z m(E) \quad (2)$$

with

$$f(k, E) = f_0(k) + f'(E) - i f''(E) \quad (3)$$

$$m(E) = m' - im''(E) \quad (4)$$

e_i and e_f are the polarization vectors of the electric field for the incident and scattered X-ray beams. E is the photon energy, k — the scattering vector and z is the unit vector along the direction of the magnetization. The regular charge scattering by the electrons of the atom, including both the form factor $f_0(k)$ and the anomalous complex contribution associated to the absorption edge, $f'(E) - if''(E)$ is given by Eq. (3). The resonant magnetic scattering factor is given by Eq. (4). Its energy dependent complex amplitude depends on the spin and orbital magnetic moments through the $F_{1,1} + F_{1,-1}$ matrix element of the dipole transition [4, 5]. It's real and imaginary parts, m' and m'' are linked by the Kramers—Kronig relation, as f' and f'' are.

3. Monte-Carlo simulations of magnetic FeRh films

To model AFM-FM phase transition in FeRh films we apply the Ising model [ref?] and perform Monte-Carlo simulations in combination with the Metropolis algorithm [5].

The Ising model is the simplest spin model, in which the spins have only two possible orientations along a chosen axis; "up" or "down". Denoting the degrees of freedom $\sigma_i = \pm 1$, the energy is

$$E = \sum_{i,j} J_{ij} \sigma_i \sigma_j - h \sum_i \sigma_i \quad (5)$$

where we have also included an external magnetic field. The interaction J_{ij} is again often (but not always) non-zero only between nearest neighbors.

The Metropolis algorithm works in the case of the Ising model, for which the energy in the presence of a magnetic field is given by Eq. (5); a configuration update amounts to selecting a spin at random and flipping it with probability (7).

$$P(C_i) = \frac{1}{Z} e^{\frac{-E(C_i)}{T}}, \quad W(C_i) = e^{\frac{-E(C_i)}{T}} \quad (6)$$

$$P^{accept}(C_i \rightarrow C_j) = \min \left[\frac{W(C_j)}{W(C_i)}, 1 \right] \quad (7)$$

When updating an Ising configuration; $C \rightarrow C'$, by flipping any number of spins, the weight ratio $W(C')=W(C)$ in the acceptance probability is given explicitly by

$$\frac{W(C')}{W(C)} = \exp \left[-\frac{J}{T} \sum_{\langle i,j \rangle} (\sigma'_i \sigma'_j - \sigma_i \sigma_j) + \frac{h}{T} \sum_i (\sigma'_i - \sigma_i) \right] \quad (8)$$

where $\{\sigma'_i\}$ are the spins of the updated configuration. Flipping a single spin j , we get

$$\frac{W(C')}{W(C)} = \exp \left[\frac{2J}{T} \sigma_j \left(\sum_{\delta[j]} \sigma_{\delta[j]} - \frac{h}{J} \right) \right] \quad (9)$$

where $\delta[j]$ denotes a nearest neighbor of site j (of which there are $2d$ on a d -dimensional cubic lattice). Since the accept/reject criterion in practice amounts to comparing the above ratio with a random number $0 \leq r < 1$, these ratios can be used directly without taking the minimum with 1, which required in the actual probability (7).

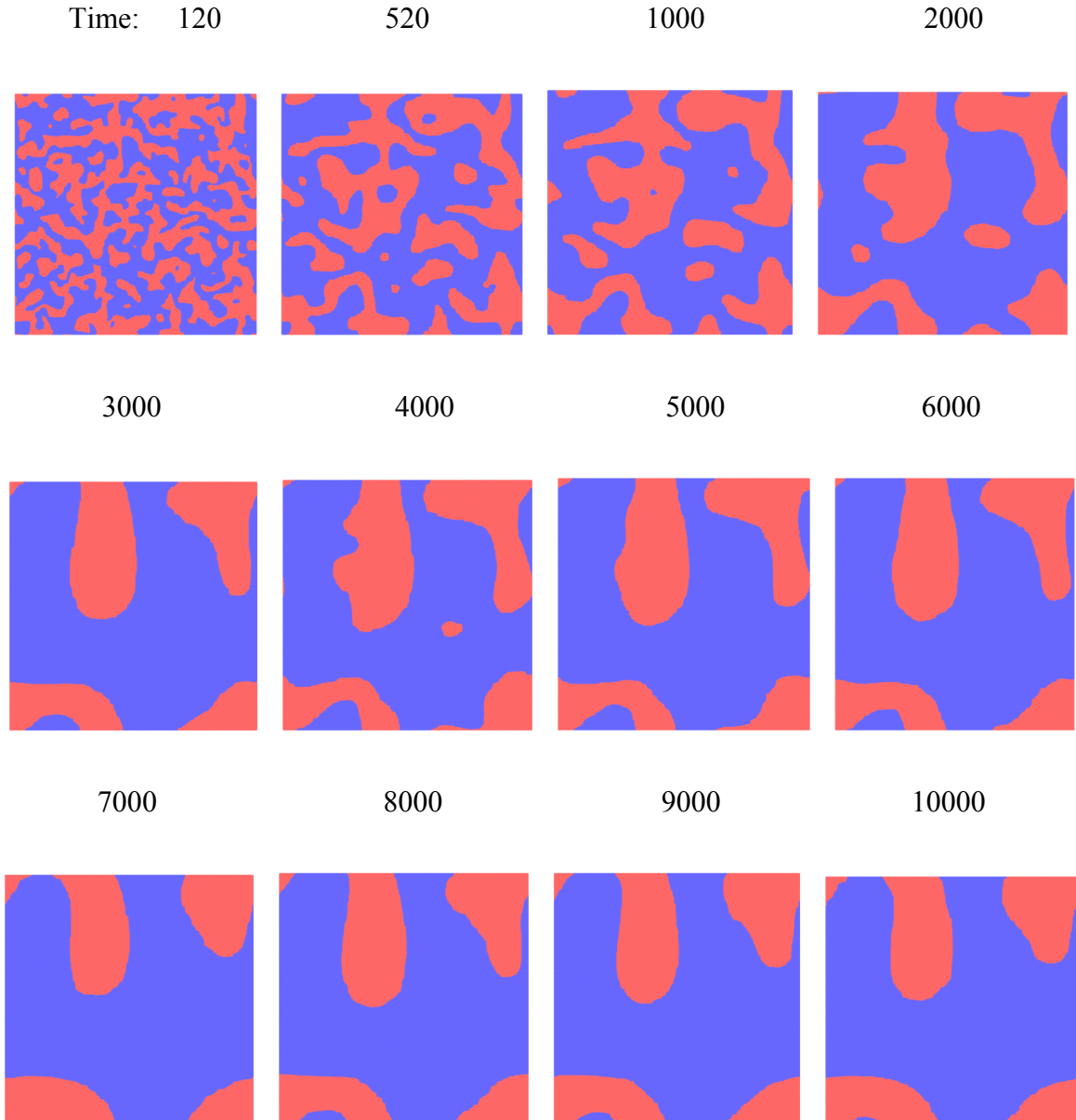


Figure 3. Example of Monte-Carlo simulation of time evolution of the correlation length

4. Results of simulations

In this work we used two different sample models to describe the time evolution of the FeRh magnetic structure.

4.1 Ising model

We simulated two-dimensional samples of 3 different sizes ($6000 \times 6000 \text{ \AA}$, $4000 \times 4000 \text{ \AA}$ and $2000 \times 2000 \text{ \AA}$), and used two methods to study evolution of the domain structure and the correlation length.

Method 1 Correlation length calculated from the simulated intensity.

After modeling magnetic scattering from our sample we calculated radial intensity profiles (Fig.4a). for all time steps of Monte-Carlo simulation. The correlation function was determined through the Fourier-transformation (FT) of intensity (Fig.4b). From fitting this correlation functions we determined the time dependence of the correlation length (Fig.5).

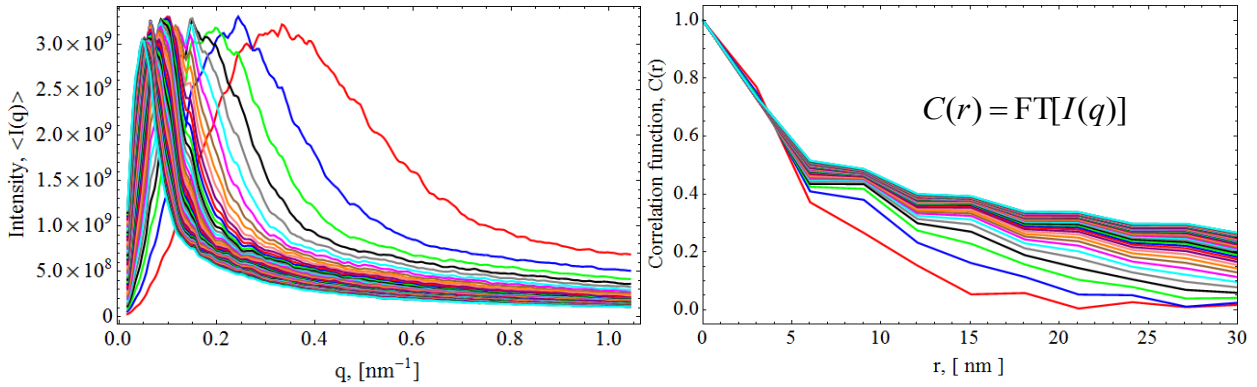


Figure 4 Intensity profiles (a) for the sample size $6000 \times 6000 \text{ \AA}$, and the corresponding correlation functions (b).

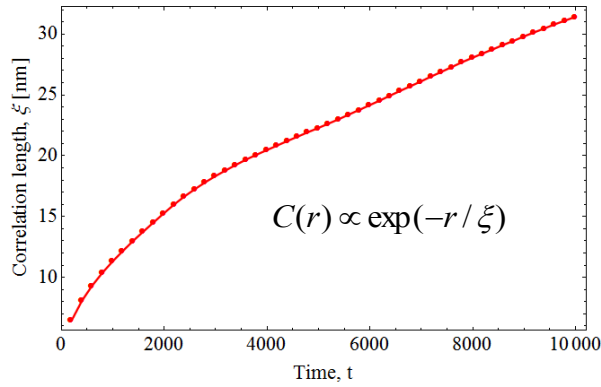


Figure 5 Correlation length determined for the sample size $6000 \times 6000 \text{ \AA}$.

Method 2 Correlation length calculated directly from the simulated sample.

The results of calculation and fitting the correlation function determined by method 2 are show in Fig.6 and Fig.7.

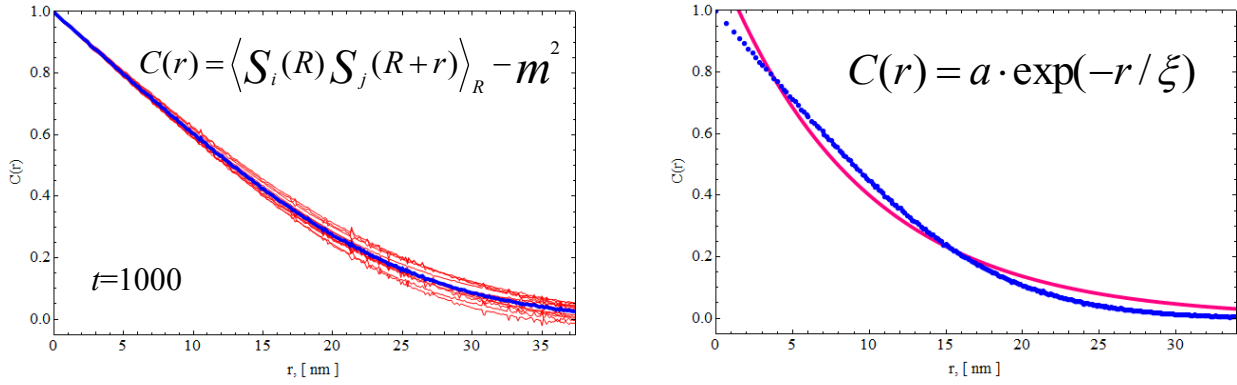


Figure 6 Averaging (a) and fitting (b) the correlation length calculated for different Monte Carlo runs (red curves) at the time step $t=1000$.

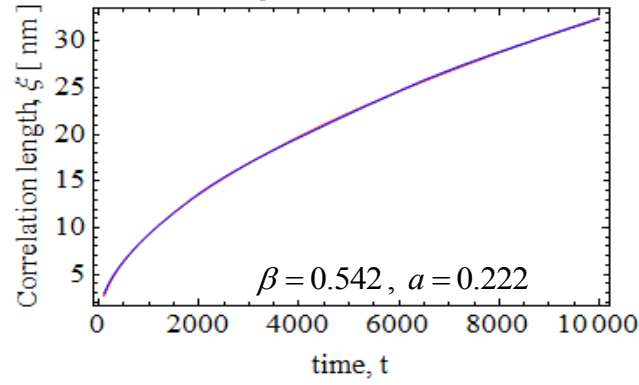


Figure 7 Time evolution of the correlation length (blue line), fitted with the function $\xi(t) = a \cdot t^\beta$ (red line).

Figure 8 shows the results of comparison of correlation length determined by two methods for the sample size $6000 \times 6000 \text{ \AA}$. Comparison of the results for different sample sizes is shown in Figure 9.

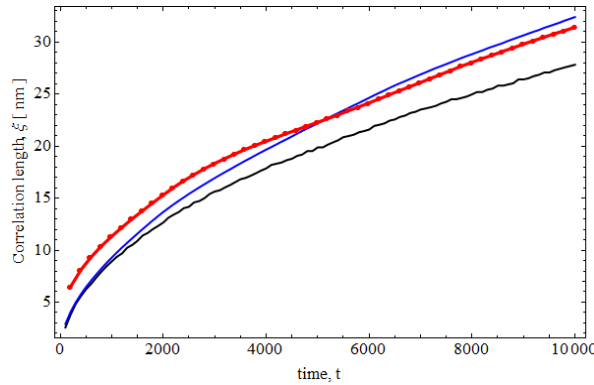


Figure 8 Comparison of correlation length determined by different calculation methods for the sample size $6000 \times 6000 \text{ \AA}$ (red - data from intensity, blue- directly from the sample by fitting, black – directly from the sample as half-width of the scattering peak).

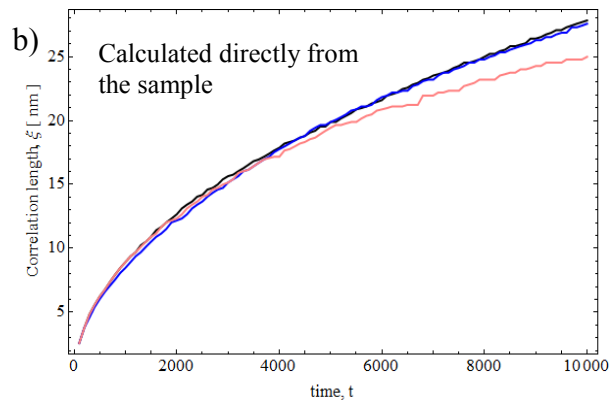
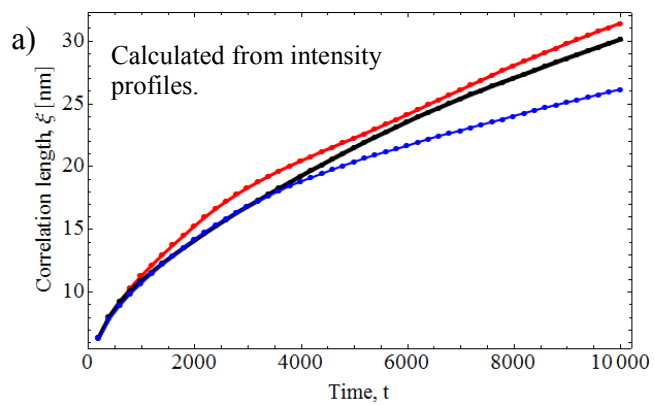


Figure 9 Comparison of the correlation length determined by different calculation methods for 3 sample sizes: a) red line – sample size $6000 \times 6000 \text{ \AA}$, black - $4000 \times 4000 \text{ \AA}$, blue - $2000 \times 2000 \text{ \AA}$; b) black line - $6000 \times 6000 \text{ \AA}$, blue - $4000 \times 4000 \text{ \AA}$, pink - $2000 \times 2000 \text{ \AA}$.

4.2 Bubble-domain model.

For bubble-domain model we used a sample with $2000 \times 2000 \text{Å}$ size and 2 different options for FM domain formation: 1) domains with spin-up and spin-down in the AFM matrix and 2) domains with spin-up only. Analysis of these data has shown qualitatively and quantitatively different evolution of the scattering profile shape and peak position during domain coarsening (see Fig.11). Comparison of these data with the experimental scattering data shows inconsistency of the second model with the real sample time evolution.

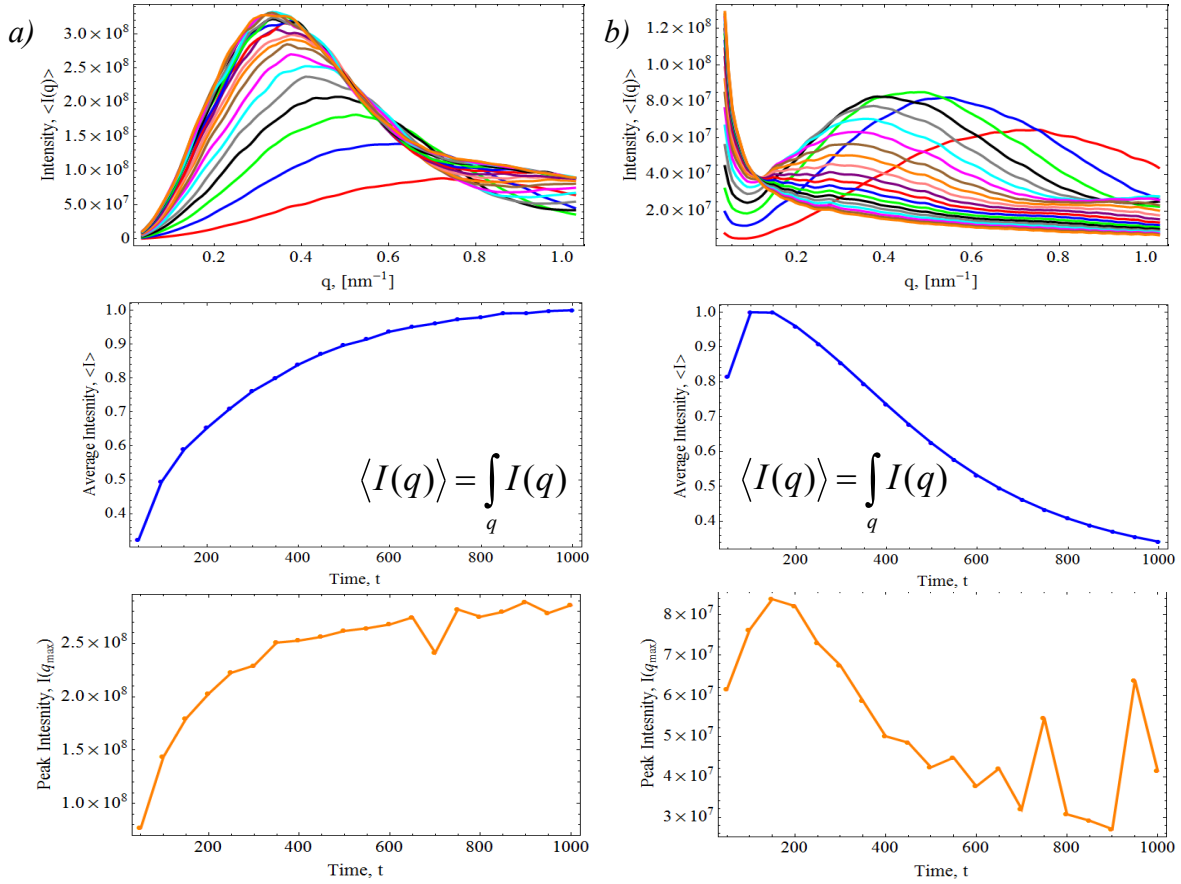


Figure 11 Radial intensity profiles, as well as average intensity and peak intensity profiles as a function of time for the samples with bubble domains with (a) spin-up and spin-down configuration, and (b) with spin-up only.

5. Conclusions

- Scattered intensity increases quadratically with the sample size.
- Statistical properties of the simulated correlation functions correlation improve with increasing of the sample size.
- At short times of Monte-Carlo simulation ($t \leq 2000$) the correlation length looks similar for all considered sample sizes within Ising model and reaches 14 nm.
- The parameter beta, that describes time evolution of the spin-spin correlation length, $\beta = 0.542$, at early times is close to the experimentally determined value.
- Bubble-domain model with spin-up domains only does not reproduce the experimentally observed features of magnetic scattering.

6. References

- [1] J.-U. Thiele, M. Buess, C.H. Back, Spin dynamics of the AF to FM phase transition in FeRh on a sub-ps time scale, *Appl. Phys. Lett.* **85**, 2857 (2004).
- [2] S. O. Mariager, F. Pressacco, G. Ingold, A. Caviezel, E. Möhr-Vorobeva, P. Beaud, S. L. Johnson, C. J. Milne, E. Mancini, S. Moyerman, E. E. Fullerton, R. Feidenhans, C. H. Back, and C. Quitmann, Structural and Magnetic Dynamics of a Laser Induced Phase Transition in FeRh, *Physical review letters*, PRL 108, 087201 (2012)
- [3] N. Metropolis, A. W. Rosenbluth, M. N. Rosenbluth, A. H. Teller, and E. Teller, Equations of state calculations by fast computing machines, *J. Chem. Phys.* 21, 1087 (1953).
- [4] J.P. Hannon, G.T. Trammell, M. Blume, D. Gibbs, *Phys. Rev. Lett.* 61, 1245 (1988).
- [5] P. Carra, M. Altarelli, *Phys. Rev. Lett.* 64, 1286 (1990).